ELSEVIER

Journal of Nuclear Materials 307–311 (2002) 941–945

journal of nuclear materials

www.elsevier.com/locate/jnucmat

Effects of dislocation on thermal helium desorption from iron and ferritic steel

R. Sugano [a], K. Morishita [a,*], H. Iwakiri [b], N. Yoshida [b]

[a] *Institute of Advanced Energy, Kyoto University, Gokasho, Uji-shi, Kyoto 611-0011, Japan*
[b] *Research Institute for Applied Mechanics, Kyushu University, Fukuoka 816-8580, Japan*

Abstract

Thermal desorption measurements were performed to investigate helium trapping in α-iron and a reduced activation martensitic steel (RAMS) bombarded at room temperature with mono-energetic He^+ ions. Incident energies were both 8 keV and 150 eV. Prior to helium implantation, the samples of α-iron were plastically deformed by rolling at room temperature followed by annealing at 673, 873 and 1073 K for 2, 12 and 2 h, respectively. These samples are hereafter called PR1, PR2 and FA, respectively, and the as-rolled sample is called CW. The dislocation densities of the samples decrease in the order of CW, PR1, PR2 and FA. Thermal desorption spectra show a clear peak at around 800 K, only for the CW, PR1, PR2 and RAMS samples, which may correspond to desorption of helium atoms trapped by dislocations. The effects of dislocations on micro-structural evolution in iron and the steel during helium implantation are discussed.

1. Introduction

The irradiation of first wall materials in a fusion reactor with 14 MeV neutrons will not only create displacement damage but also generate hydrogen and helium at high rates [1]. Especially for helium, it seems to be inevitable that it will precipitate as bubbles at relatively high temperatures, since it is insoluble in most metals and alloys [2]. The existence of helium bubbles in metals may have a great impact on changes in the microstructure and corresponding mechanical property of irradiated materials.

Reduced activation martensitic steels (RAMS) are one of the promising candidate alloys for the first wall of fusion reactors, because they possess high swelling resistance, high strength, and low activation [3]. It is reported that, even considering helium effects, the steel is not inappropriate as a first wall material [4]. This is probably because there are a lot of trapping sites for helium atoms, preventing helium from clustering as a bubble. The clustering may affect the properties of the material. These trapping sites in the steel are considered to be dislocations, the interface of precipitates and lath boundaries. In order to use their function to prevent helium from clustering in the steel, we must investigate the strength of binding between these trapping sites and helium atoms, or dissociation temperatures between them, which may provide the upper limit of temperature where the steel can be utilized without helium clustering. In the present study, the binding states and strength between dislocations in the steel and helium atoms were investigated using a thermal desorption spectrometry (TDS) technique applied to cold-worked pure iron and RAMS that were irradiated by energetic helium ions.

2. Experimental procedure

In the present work, we used samples of pure iron and reduced activation martensitic steels (JLM-1). The

* Corresponding author. Tel.: +81-774 38 3477; fax: +81-774 38 3479.
E-mail address: morishita@iae.kyoto-u.ac.jp (K. Morishita).

0022-3115/02/$ - see front matter
PII: S0022-3115(02)01098-X

Table 1
Chemical composition (mass%) and heat treatment of JLM-1 and pure-Fe used in the present study. Heat treatments of JLM-1: normalized at 1323 K for 30 min and then tempered at 1033 K for 1 h, followed by air cooling

	C	Si	Mn	P	S	Cr	V	Ti	W	Ta	B	O	N
JLM-1	0.10	0.042	0.53	0.002	0.0014	9.03	0.26	0.021	2.06	0.051	0.0032	–	–
Pure-Fe	0.001	–	–	–	–	–	–	–	–	–	–	0.005	0.001

chemical composition of the samples used in this work is given in Table 1. The ingots of pure iron (99.99%) were, at first, cold rolled to sheets of approximately 0.2 mm thickness, cut into 5×10 mm^2 pieces, and chemically polished in a solution of 5%-HF and 95%-H_2O_2. After these processes, the samples were annealed at the temperatures of 673, 873, 1073 K for 2, 12, and 2 h under high vacuum condition (10^{-6} Pa), respectively. For these temperatures, monovacancies in the samples annealed out since the temperatures were above annealing stage V. The samples are, hereafter, called PR1, PR2 and FA, respectively, and the as-rolled sample is indicated by CW. The Vickers hardnesses of the samples were different depending on the thermal treatment: it was 180, 110, 74 and 62 for the CW, PR1, PR2 and FA samples, respectively. The difference in the hardness may reflect the difference in the density of dislocations in the samples. Dislocation densities estimated from the Vickers hardness measurements are 3×10^{14}, 5×10^{13}, and 3×10^{12} m^{-2} for the CW, PR1, PR2 samples, respectively. The grain sizes of the samples were also different: they ranged from 1 to 100 μm and increased in order of FA, PR2, PR1 and CW.

The samples were bombarded at room temperature with collimated, mass-analyzed beams of mono-energetic He^+ ions. The irradiation dose of incident helium ions ranged from 2×10^{17} He^+/m^2 to 6×10^{19} He^+/m^2, with a fixed dose rate of about 1×10^{17} $He^+/m^2/s$. The energies of the incident ions were 8 keV and 150 eV, where atomic displacement damage does and does not take place in iron, respectively. TRIM [5] calculations indicate that these energies correspond to the approximate helium maximum penetration depth of 100 and 10 nm, respectively. For 8 keV irradiations, displacement damage ranges over 100 nm with a peak at 25 nm from the surface, producing 6×10^{-4} displacements per atom (NRT-dpa) at the peak for 1×10^{17} He^+/m^2.

After the irradiations, the samples were heated up to 1500 K by infrared irradiation. The ramping rate of the temperature was fixed at 1 K/s. During heating, helium release was monitored by a quadrupole mass analyzer and background vacuum was kept at the magnitude of 10^{-5} Pa. The total amount of desorbing helium atoms detected during heating to 1500 K was almost the same as the amount of helium atoms implanted into the samples.

3. Results and discussion

3.1. Helium desorption from pure iron irradiated by 150 eV He ions

Fig. 1 indicates the thermal helium desorption spectra of the samples irradiated by 150 eV He^+ ions at room

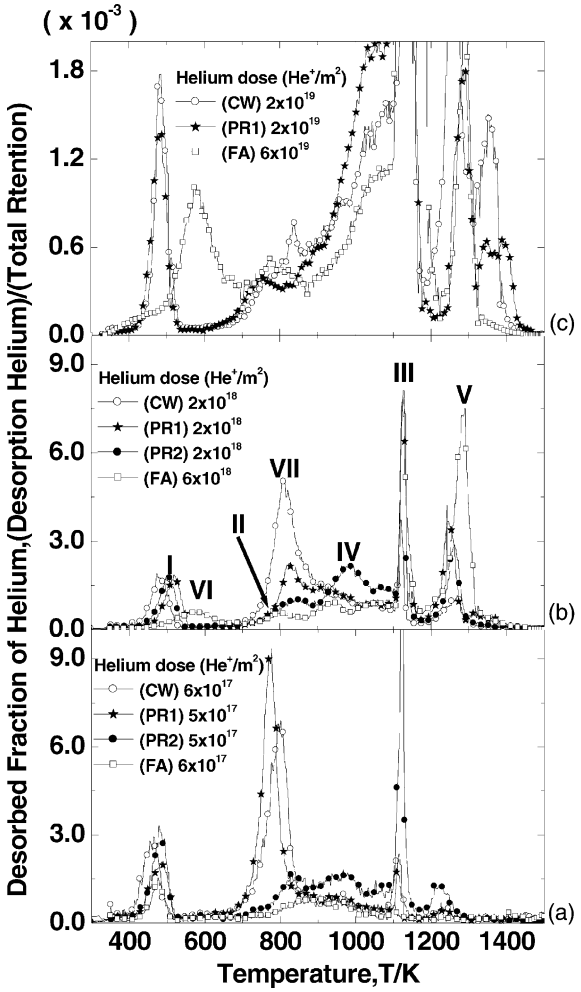

Fig. 1. Helium desorption spectra of (a) 10^{17} He^+/m^2, (b) 10^{18} He^+/m^2 and (c) 10^{19} He^+/m^2 150 eV helium implanted into deformed α-iron, which are called as CW, PR1, PR2 and FA.

temperature as a function of irradiation dose for the samples. At the lowest dose, as shown in Fig. 1(a), the helium desorption spectrum for the FA sample shows a sharp peak at 450 K, broad peaks ranging between 650 and 1000 K, and another sharp peak at 1100 K. These peaks are, hereafter, called as peaks I, IV and III, respectively. At higher doses for the FA sample, in addition to the desorption peaks described above, two peaks appeared at around 550 K and greater than 1250 K, and peak IV divided into two parts; one was a sharp peak at about 800 K and the other was a broad peak ranging between 800 and 1000 K. These peaks are called VI, V, II and IV, respectively. On the other hand, for the CW, PR1 and PR2 samples, peaks I, III, IV and V appeared as shown in Fig. 1(a), as well as a new sharp peak at about 800 K that is observed for all of the irradiation doses. This peak is, hereafter, called peak VII.

Peaks I, II, III, IV, V and VI are considered to be ascribed to helium desorbing from multiply filled and singly filled vacancies and their clusters, as discussed elsewhere [6]. Our calculation shows that helium binding energy to the helium-vacancy cluster ranges from 1.8 to 5.3 eV, depending on the helium-to-vacancy ratio of the cluster [7]. On the other hand, the amount of helium at peak VII increases with increasing helium implantation dose and it is finally saturated at the highest dose of about 10^{19} He/m^2. In addition, with increasing dose, the peak VII temperature is shifted higher. This behavior of helium desorption is definitely different from that of desorption at peak II (desorption from vacancy-related defects) that is gradually shifted to lower temperature at higher dose. Moreover, at the fixed implantation dose investigated here, the height of peak VII decreases and the peak VII temperature increases in the order of CW, PR1, PR2 and FA. Since this peak is not considered to correspond to dissociation of helium atoms from vacancy-related defects, it may be attributed to helium desorption from the defects that are produced or changed during the plastic deformation and subsequent heat treatments before the helium implantation. These defects are essentially dislocations and grain boundaries.

Berg et al. [8] performed atomistic calculations, showing that the energy for dissociation of a single helium atom from a $1/2\langle 1\,1\,1\rangle\{1\,1\,0\}$ edge dislocation or from a small helium cluster (number of helium atoms up to 4) bound to the dislocation is about 2.3 eV. In the absence of information on the binding states between a helium atom and a screw dislocation, the desorption temperature of peak VII is in good agreement with their calculated energy. Therefore, one of the possible desorption mechanisms at peak VII may be ascribed to helium desorption from dislocations. Butters et al. [9–11] reported that helium desorption from dislocations was not observed in cold-worked single crystal molybdenum irradiated by 150 eV helium ions. They pointed out that all the helium atoms once trapped by a dislocation migrate very rapidly along the dislocation to a surface due to pipe diffusion, resulting in no production of helium clusters bound to dislocations. If pipe diffusion is also dominant in our samples, a fraction of helium atoms should escape during irradiation, because the helium-implanted depth is much smaller than the grain size and therefore dislocations reach not only grain-boundaries but also the surface. But it is inconsistent with our observation. Implanted helium atoms even in our cold-worked samples were all retained in the samples before the TDS measurements. Since one expects that dislocations have a lot of jogs and vacancies, which prevent helium pipe diffusion [12], it is not unreasonable to consider that helium atoms are trapped in a cluster bound to dislocations, and that they desorb from dislocations at peak VII temperatures.

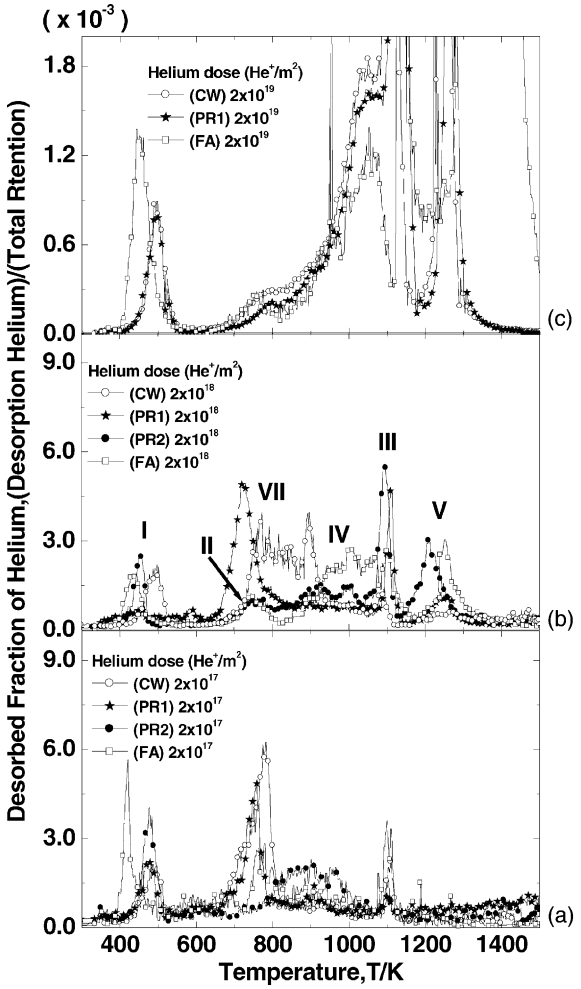

Fig. 2. Helium desorption spectra of (a) 10^{17} He$^+$/m^2, (b) 10^{18} He$^+$/m^2 and (c) 10^{19} He$^+$/m^2 8 keV helium implanted into deformed α-iron, which are called as CW, PR1, PR2 and FA.

The other possible mechanism for peak VII is desorption of helium from grain boundaries. Our spectra show that the amount of helium atoms desorbing at peak VII increases with decreasing grain size. Which desorption mechanism is dominant at peak VII, dislocation trap, grain boundary trap or both, is not clear at present.

In general, vacancies bound to dislocations and grain boundaries can diffuse very rapidly. Therefore, when implantation dose increases and helium atoms are accumulated at the dislocations or grain boundaries, a helium-vacancy cluster on these defects accumulates vacancies very easily to relax the compressive strain produced by the cluster. It results in an effective decrease in the helium-to-vacancy ratio of the cluster and therefore an increase in the binding energy of helium to a cluster, which leads to the peak VII shift to higher temperatures as described above.

3.2. Helium desorption from pure iron irradiated by 8 keV He ions

Fig. 2 indicates the thermal helium desorption spectra of the samples irradiated by 8 keV He^+ ions at room temperature as a function of irradiation dose. Peaks I, II, III, IV, V and VII were also observed at the 8 keV irradiations, as shown in Fig. 2. The amount of helium desorbing at peak VII was smaller in the 8 keV irradiations than in the 150 eV irradiations. This is probably because, different from the 150 eV irradiations, energetic incident helium ions of 8 keV produce atomic displacement damage to create a large number of vacancies where most of the helium atoms are preferentially trapped by vacancies and their clusters, and therefore, the number of helium atoms bound to dislocations or grain boundaries decreases.

3.3. Helium desorption from JLM-1

Figs. 3 and 4 indicate the thermal helium desorption spectra obtained from the JLM-1 steel and pure-iron

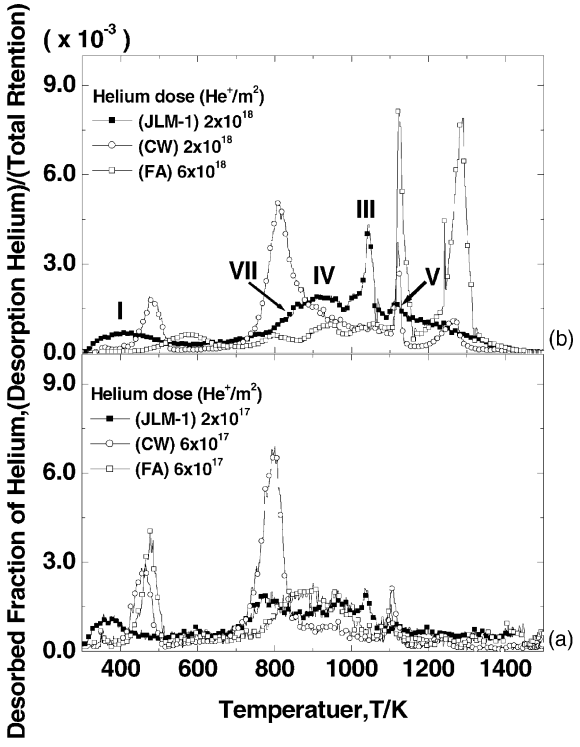

Fig. 3. Helium desorption spectra of (a) 10^{17} He^+/m^2 and (b) 10^{18} He^+/m^2 150 eV helium implanted into the deformed α-iron (CW and FA) and the JLM-1.

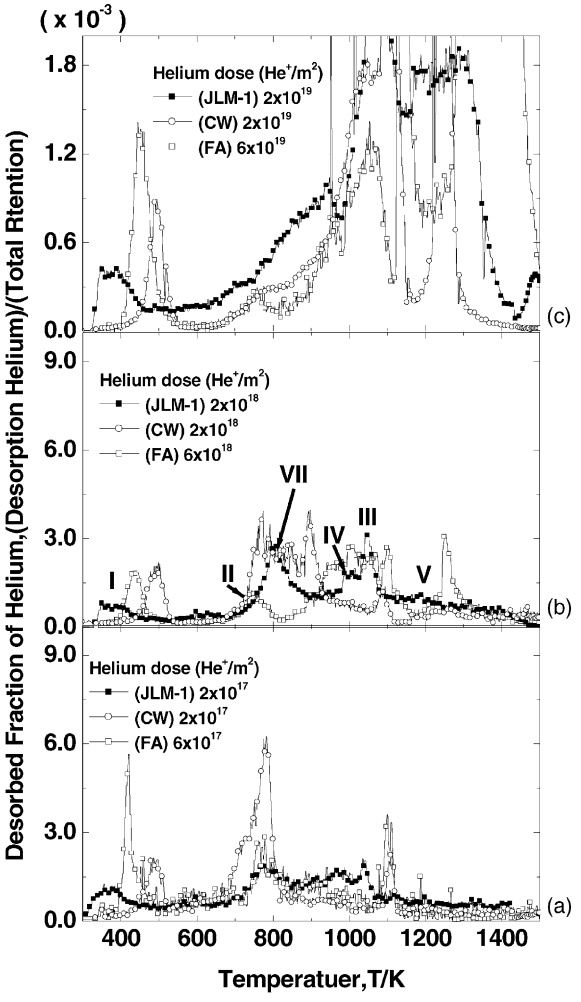

Fig. 4. Helium desorption spectra of (a) 10^{17} He^+/m^2, (b) 10^{18} He^+/m^2 and (c) 10^{19} He^+/m^2 8 keV helium implanted into deformed α-iron (CW and FA) and the JLM-1.

(CW and FA) irradiated by 150 and 8 keV He^+ ions at room temperature as a function of irradiation dose. Peaks I, II, III, IV, V and VII were also observed in the helium desorption spectra of the JLM-1 steel.

Peak VII, representing dissociation of helium atoms from dislocations or grain boundaries, was also observed in the spectra of the steel, indicating that some of the helium atoms are also trapped at dislocations and grain boundaries in the steel. As shown in the desorption spectra of iron, the amount of helium desorption at peak VII decreases with increasing incident He energy in the steel. Irrespective of the highest dislocation density ($\sim 10^{15}$ m^{-2}) and the smallest grain (subgrain) size, the amount of helium trapped at the dislocations and grain boundaries (peak VII) in the JLM-1 steel is smaller than that of the CW sample. This indicates that there are many defects to trap helium in the steel, in addition to vacancies, dislocations and grain boundaries. One expects that these defects can trap helium atoms to prevent them from clustering, depending on their own binding strength. For example, dislocations and grain boundaries can trap helium below 800 K, which would be the upper limit of the temperature where the steel can be utilized without helium clustering attributed to dislocations. Further investigation is required to know the binding states and strength of helium for the other defects.

4. Conclusions

Thermal desorption measurements were performed to investigate helium entrapment in cold-worked and annealed α-iron and a RAMS (JLM-1). The helium desorption peak associated with dislocations was observed at approximately 800 K. So many defects (vacancies, dislocations, grain boundaries, lath-boundary, carbides.) are included in the steel and they trap and disperse helium atoms to prevent them from clustering as a bubble.

Acknowledgements

The authors wish to acknowledge the collaboration program provided by Research Institute for Applied Mechanics, Kyushu University. The part of this work was supported by a Grant-in-Aid from the Ministry of Education, Culture, Sports, Science and Technology of Japan, and the part of the work was performed under the auspices of Japan Nuclear Cycle Development Institute.

References

[1] B.N. Singh, T. Leffers, J. Nucl. Mater. 125 (1984) 287.
[2] M. D'Olieslaeger, G. Knuyt, L. De Schepper, L.M. Stals, Theoretical description of the growth and stability of helium platelets in nickel, in: S.E. Donnelly, J.H. Evans (Eds.), Fundamental Aspects of Inert Gas in Solids, Plenum, 1991, p. 27.
[3] A. Kohyama, A. Hishinuma, D.S. Gelles, R.L. Klueh, W. Dietz, K. Ehrlich, J. Nucl. Mater. 233–237 (1996) 138.
[4] R. Lindau et al., J. Nucl. Mater. 271&272 (1999) 450.
[5] J.P. Biersack, L.G. Haggmark, Nucl. Instrum. and Meth. B 2 (1984) 814.
[6] K. Morishita, R. Sugano, H. Iwakiri, N. Yoshida, A. Kimura, in: Proceedings of Fourth Pacific Rim International Conference on Advanced Materials and Processing, Honolulu, Hawaii, USA, J. Jpn. Inst. Met. 1 (2001) 1395.
[7] K. Morishita, B.D. Wirth, T. Diaz de la Rubia, A. Kimura, in: Proceedings of Fourth Pacific Rim International Conference on Advanced Materials and Processing, Honolulu, Hawaii, USA, J. Jpn Inst. Met. 1 (2001) 1383.
[8] F.v.d. Berg, W.v. Heugten, L.M. Caspers, A.v. Veen, Solid State Comm. 24 (1977) 193.
[9] W.Th.M. Buters, A. van den Beukel, J. Nucl. Mater. 137 (1985) 57.
[10] W.Th.M. Buters, A. van den Beukel, J. Nucl. Mater. 141–143 (1986) 253.
[11] W.Th.M. Buters, A. van den Beukel, J. Nucl. Mater. 144 (1987) 71.
[12] F.v.d. Berg, W.v. Heugten, L.M. Caspers, A.v. Veen, Solid State Commun. 27 (1978) 665.